

Low-Energy Properties of Realistic N - N One-Boson-Exchange Potentials

ALEXANDER GERSTEN AND A. E. S. GREEN
University of Florida, Gainesville, Florida 32601
 (Received 29 July 1968)

We examine the low-energy features of the N - N interaction, as described by three realistic one-boson-exchange potential models. These models are the Green-Sawada two-parameter model, the Bryan-Scott III model, and the Ueda-Green I model. We calculate the deuteron binding energy, wave functions, magnetic and quadrupole moments, effective range, and electromagnetic form factors. Where possible, these quantities are compared with the experimental data.

1. INTRODUCTION

VERY recently, one-boson-exchange potentials (OBEP) have been developed which describe all phenomenological N - N phase shifts quite accurately, including S waves.¹⁻⁵ It is therefore possible to examine in detail the low-energy properties of such realistic OBEP with the objective of furthering our understanding of the N - N interaction, which is of such fundamental importance to nuclear physics. We shall confine our discussions to the models of Green and Sawada, particularly their simple two-parameter model,³ which is fairly representative of their more precise seven-parameter models,² the Bryan-Scott (BS) III model,⁴ and the Ueda-Green (UG) I model.⁵ The last model, which has been adjusted to the most recent N - N phase shifts,^{6,7} will be given the greatest attention.

These models are based upon the exchange of pseudoscalar (P), vector (V), and scalar (S) mesons and all lead to a total potential V_{tot} of the form given by Eq. (16) and Table I of Ref. 5. All of these studies use generalized Yukawa potentials which are special cases of the "well-regulated" potential of Green and Sawada [see Eq. (3.15) of Ref. 3] with the regulators Λ and U . In the Green-Sawada two-parameter model, $U \equiv 20M_\pi$, $\Lambda_\pi \equiv M_\omega$, and for all other regulators $\Lambda = 1500 \text{ MeV}^*$. In the Bryan-Scott model, $U \equiv \infty$, and all $\Lambda = 1500 \text{ MeV}^*$. In the (UG) I model, $\Lambda_\pi = U_\pi = 2532 \text{ MeV}^*$ and for all other mesons $\Lambda = U = 1185 \text{ MeV}^*$ (the constants with asterisks denote adjusted parameters). The parameters of those models are summarized in Table I. Elsewhere,⁸ several general features of realistic OBEP have been examined. Here we concentrate on low-energy features and our calculations give the following deuteron quanti-

ties: wave functions, binding energy, magnetic and quadrupole moments, effective-range parameters, and electromagnetic form factors. We hope that these calculations will give a further check on the validity of these OBEP, will guide further development of OBEP, and will furnish additional information of importance to studies of nuclear physics.

2. DEUTERON GROUND STATE

Our task is to find the ground-state solution to the Schrödinger equation

$$(\nabla^2 - \gamma^2 - v_{\text{tot}})\Psi = 0, \quad (1)$$

where

$$v_{\text{tot}} = MV_{\text{tot}}/\hbar^2, \quad \gamma^2 = M\epsilon/\hbar^2,$$

where V_{tot} is the nucleon-nucleon potential, ϵ is the binding energy, and M is the nucleon mass. We assume that the deuteron wave function is combined from wave functions of the 3S_1 and 3D_1 states in the usual way, i.e.,

$$\Psi = [u(r)Y_{00}^m + w(r)Y_{21}^m]/r, \quad (2)$$

where Y_{LSJ}^m is the normalized eigenfunction of the J^2 operator obtained by coupling the eigenfunctions of the L^2 and S^2 operators and m is the magnetic number.

All of the realistic OBEP have velocity-dependent terms of the form $V_p(r)p^2 + p^2V_p(r)$. To eliminate the first-derivative terms in the coupled differential equation we substitute in (2) and (1)

$$\begin{aligned} u(r) &= y(r)[1 + \phi(r)]^{-1/2}, \\ w(r) &= z(r)[1 + \phi(r)]^{-1/2}, \end{aligned} \quad (3)$$

TABLE I. Mesons and coupling constants.

Meson	T, J^P	Mass (MeV)			Coupling constants		
		GS I	BS III	UG I	GS 2	BS III ^a	UG I ^a
π	1, 0 ⁻	138.7	138.7	138.7	14.7	12.658 ^b	14.10
η	0, 0 ⁻	548.7	548.7	548.7	...	3.002 ^b	4.430 ^b
ω	0, 1 ⁻	782.8	782.8	782.8	23.0 ^b	23.72	25.24 ^b
ρ	1, 1 ⁻	763	763	763	0.65	2.442 ^b	2.272 ^b
f/g					(3.75)	(1.13) ^b	(4.76)
σ	0, 0 ⁺	782	550 ^b	1070	14.7	9.462	133.1 ^b
σ_1	1, 0 ⁺	763	600 ^b	1016	0.65	1.964 ^b	58.57 ^b
σ_c	0, 0 ⁺	416		416	2.35		2.551 ^b

^a To compare the various models we refer to $[\Lambda^2/(\Lambda^2 - m^2)]g^2$ as the coupling constant for the BS III model and $[\Lambda^2/(\Lambda^2 - m^2)]g^2$ as the coupling constant for the UG I model.

^b Denotes adjustable constants.

* Supported in part by the U. S. Air Force Office of Scientific Research.

¹ A. E. S. Green and T. Sawada, Nucl. Phys. **B2**, 276 (1967).

² A. E. S. Green and T. Sawada, Rev. Mod. Phys. **39**, 594 (1967).

³ A. E. S. Green and T. Sawada, Contributions to International Conference on Nuclear Structure, Tokyo, Japan, 1967, Sec. 3.5 (unpublished).

⁴ R. A. Bryan and R. L. Scott (unpublished).

⁵ T. Ueda and A. E. S. Green, Phys. Rev. **174**, 1304 (1968).

⁶ G. Breit *et al.*, Phys. Rev. **165**, 1579 (1968).

⁷ M. H. MacGregor *et al.*, University of California Laboratory Report No. UCRL-70075 (Part IX), 1968 (unpublished).

⁸ T. Sawada, A. Dainis, and A. E. S. Green, Phys. Rev. (to be published).

TABLE II. Deuteron wave functions of the UG model.

r (F)	$u(r)$	$w(r)$	r (F)	$u(r)$	$w(r)$
0.2	0.0274	0.0147	4.2	0.3377	0.0543
0.4	0.1056	0.0588	4.4	0.3234	0.0497
0.6	0.2073	0.0984	4.6	0.3095	0.0456
0.8	0.3113	0.1261	4.8	0.2962	0.0419
1.0	0.3980	0.1447	5.0	0.2835	0.0386
1.2	0.4583	0.1552	5.2	0.2712	0.0355
1.4	0.4936	0.1584	5.4	0.2595	0.0327
1.6	0.5097	0.1558	5.6	0.2483	0.0302
1.8	0.5128	0.1493	5.8	0.2375	0.0279
2.0	0.5074	0.1406	6.0	0.2272	0.0258
2.2	0.4967	0.1309	6.2	0.2173	0.0239
2.4	0.4830	0.1208	6.4	0.2078	0.0221
2.6	0.4674	0.1110	6.6	0.1988	0.0205
2.8	0.4509	0.1017	6.8	0.1901	0.0191
3.0	0.4340	0.0930	7.0	0.1818	0.0177
3.2	0.4171	0.0849	7.2	0.1739	0.0165
3.4	0.4004	0.0776	7.4	0.1663	0.0154
3.6	0.3840	0.0709	7.6	0.1591	0.0143
3.8	0.3681	0.0648	7.8	0.1521	0.0133
4.0	0.3526	0.0593	8.0	0.1455	0.0124

where $\phi(r) = 2V_p(r)/a$ and $a = \hbar/Mc$. Then Eq. (2) transforms into the coupled equations

$$y''(r) - [\gamma^2 + v_0(r)]y(r) = \sqrt{8}v_T(r)(1+\phi)^{-1}z(r),$$

$$z''(r) - [\gamma^2 + 6r^{-2} + v_2(r)]z(r) = \sqrt{8}v_T(r)(1+\phi)^{-1}y(r),$$

where

$$v_0(r) = [1 + \phi(r)]^{-1} \times [v_c(r) + v_\sigma(r) - \gamma^2\phi + (\nabla\phi)^2/4(1+\phi)]$$

and

$$v_2(r) = v_0 - [3v_{LS}(r) + 2v_T(r)]/(1+\phi).$$

We look for a solution to (4) satisfying

$$y(0) = y(\infty) = z(0) = z(\infty) = 0.$$

Under these conditions, the asymptotic behavior of the solutions to (4) is given by

$$u(r) \sim y(r) \sim Ne^{-\gamma r},$$

$$w(r) \sim z(r) \sim NAe^{-\gamma r} [1 + 3/\gamma r + 3/(\gamma r)^2],$$

where N is a normalization constant and the asymptotic solutions are chosen to correspond to exact solutions when $\phi(r)$, $v_2(r)$, and $v_T(r) = 0$, since these functions vanish exponentially. The constant A is introduced here because the two solutions are not independent of each other. We start to solve Eq. (4) numerically from radius $r = R$ for which we can neglect the potential. In the neighborhood of this radius, we assume that $y(r)$ and $z(r)$ have the values given by Eq. (8). Next we solve (4), using the extrapolation difference approximation of Milne⁹ beginning from $r = R$ towards $r = 0$. If we use an extrapolation scheme, we get finite values for $y(0)$ and $z(0)$ which depend on the values of γ and A assumed for Eq. (8). We solve

$$y(0; \gamma, A) = 0, \quad z(0; \gamma, A) = 0$$

by Newton's iteration method.

⁹ W. E. Milne, Am. Math. Monthly 40, 322 (1933).

We normalize our wave function according to

$$\int_0^\infty (u^2 + w^2) dr = \int_0^\infty \frac{y^2 + z^2}{1 + \phi} dr = 1.$$

We use the numerical solution for y and z between $r = 0$ and R and evaluate the integral numerically. For $r > R$, we can neglect ϕ against 1 and assume that $y(r) = u(r)$ and $z(r) = w(r)$, and that they are given by Eq. (8). Under these assumptions the contributions to the normalization integral for $r > R$ may be evaluated analytically in terms of the exponential integral $E_n(z)$.¹⁰ We also shall use the alternative normalization

$$N_\sigma^2(u^2 + w^2) \sim e^{-2\gamma r}.$$

It is easy to show, using Eq. (8), that $N_\sigma^2 = 1/[(1 + A^2) \times N^2]$. The usual D -state probability is given by

$$P_D = \int_0^\infty w^2 dr.$$

The numerical solutions of the wave functions for UG I are given in Table II. The values of the binding energy, γ , A , N_σ , and P_D for Green-Sawada (GS) 2, BS III, and UG I are given in Table III.

The UG wave functions are graphed in Fig. 1. For comparison, we show the Hamada-Johnston wave functions.¹¹ Note that they are very similar except in the core region. The BS III model (not shown) is quite close to UG I. The GS 2 model (not shown), however, departs more appreciably primarily because its binding energy is too large and hence its so-called deuteron radius γ^{-1} is too small.

The w wave functions of UG I and BS III are quite close to each other. They are smaller than the w wave function of Hamada and Johnston, which leads to the D -state probability of 6.97%.

In Fig. 2 we give the radial dependence of the deuteron density $[u(r)]^2 + [w(r)]^2$ and the quadrupole density $[uw - (w^2/\sqrt{8})]r^2$.

TABLE III. Effective-range parameters in F.

Quantity	GS 2	BS III	UG I	Expt. ^a
$\rho(-\epsilon, -\epsilon)$	1.71	1.70	1.82	1.82±0.05
a_s	-13.5	-22.7	-23.8	-23.68±0.028
a_t	4.68	5.39	5.69	5.399±0.011
r_{0s}	2.85	2.60	2.68	2.46±0.12
r_{0t}	1.72	1.69	1.82	
a_{0p}	-6.90	-8.58	-9.08	-7.80
r_{0p}	2.75	2.51	2.59	2.65
a_{0p}	6.92	-8.54	-9.12	-7.80
r_{0p}	2.75	2.50	2.58	2.65

^a Reference 13.

¹⁰ For the methods of computation of $E_n(z)$ see M. Abramowitz and I. A. Stegun, *Handbook of Mathematical Functions* (Dover Publications, Inc., New York, 1956).

¹¹ T. Hamada and I. D. Johnston, Nucl. Phys. 34, 382 (1962).

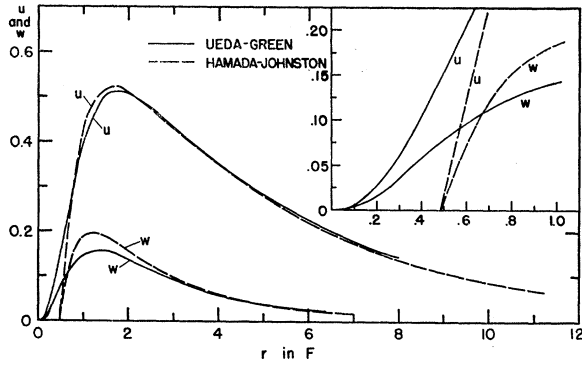


FIG. 1. Normalized deuteron wave functions $u(r)$ and $w(r)$ of the UG I models compared with the Hamada-Johnston wave functions.

3. EFFECTIVE-RANGE EXPANSIONS

It has been shown by Sawada *et al.*⁸ that the usual effective-range theory can be applied to velocity-dependent OBEP provided that regularized potentials (regular at the origin) are used. To determine the effective range and scattering lengths, phase shifts were evaluated¹² at several low energies and the first two terms in the expansion of $k \cot \delta$ in k^2 were evaluated numerically. For the most part the notation is standard¹³ and the theory is similar to that described by Hulthén and Sugawara.¹⁴

For the 3S_1 phase shift we may relate the effective-range parameters to the deuteron binding energy and mixing parameter ϵ_g in the usual way, i.e.,

$$\gamma = \frac{1}{a_t} + \frac{\gamma^2}{2 \cos \epsilon_g} \rho(0, -\epsilon). \quad (13)$$

Knowing the deuteron wave functions, we can compute

$$\rho(-\epsilon, -\epsilon) = \gamma^{-1} - 2/N\sigma^2. \quad (14)$$

In the case of p - p scattering, in addition to the N - N interaction, the Coulomb interaction e^2/r is added and the p - p effective-range representation of the calculations is obtained.¹⁵ The parameters are given in Table III. We have also computed the p - p effective-range parameters, assuming electrostatic potential of the form¹⁶ $e^2(1 - e^{-\omega r})/r$, where ω is the inverse Compton wavelength of the ω meson, which is characteristic for the nucleon electromagnetic form factor. We found that the subtractive term hardly affects the effective-range parameters.

¹² T. Sawada and A. E. S. Green, A Fortran Program for the Computation of N - N Phase Shifts, N-M-15, 1968 (unpublished).

¹³ R. Wilson, *The Nucleon-Nucleon Interaction* (Interscience Publishers, Inc., New York, 1963).

¹⁴ L. Hulthén and M. Sugawara, in *Handbuch der Physik*, edited by S. Flügge (Springer-Verlag, Berlin, 1957), Vol. 39, p. 1.

¹⁵ G. Breit, E. U. Condon, and R. D. Present, *Phys. Rev.* **50**, 825 (1936).

¹⁶ B. Podolsky, *Phys. Rev.* **62**, 68 (1942).

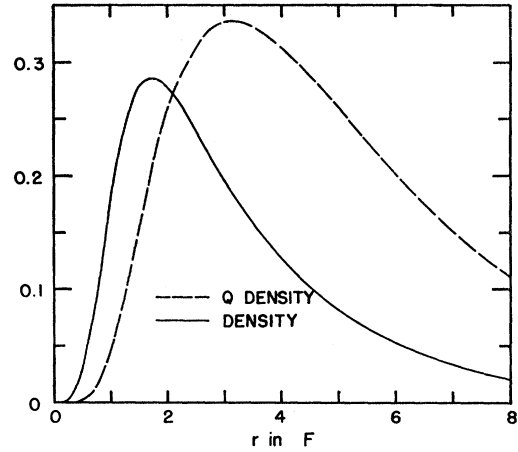


FIG. 2. Deuteron density and quadrupole density (denoted in the graph as Q density) obtained from the UG I model.

4. DEUTERON MAGNETIC MOMENT

In the absence of the spin-orbit term $V_{LS}(r)$ and the velocity-dependent potential $V_p(r)$, the magnetic moment of the deuteron is equal (in nucleon magnetons) to

$$\mu_0 = (1 - P_D)\mu_s + \frac{1}{2}(\frac{3}{2} - \mu_s)P_D, \quad (15)$$

where μ_s is the magnetic moment for a pure 3S_1 state: $\mu_s = \mu_n + \mu_p = 0.87960 \mu_N$. Here μ_n and μ_p are the magnetic moments of the neutron and proton, respectively.

In the presence of V_{LS} and V_p in the total potential new terms appear in addition to (15) and the deuteron magnetic moment has the approximate form $\mu_d = \mu_0 + \Delta\mu_{LS} + \Delta\mu_p$, where¹⁷⁻¹⁹

$$\Delta\mu_{LS} = \frac{M}{6} \int r^2 (u^2 - 2^{-1/2}uw - w^2) V_{LS}(r) dr \quad (16)$$

and

$$\Delta\mu_p = \frac{3}{4M} \int V_p(r)w^2 dr = \frac{3}{8} \int \phi(r)w^2 dr. \quad (17)$$

Here $\hbar = c = 1$ and all integrals go from 0 to ∞ .

In Table IV we see that the state probabilities P_D are very close to each other (about 5.5%) in all three realistic OBEP. The magnetic moment μ_0 , calculated without the spin-orbit and velocity-dependent correc-

TABLE IV. Deuteron parameters.

Model	ϵ_B	γ^{-1} (F)	A	$N\sigma^{-2}$	P_D
GS 2	3.36	3.52	0.0340	1.108	5.59%
BS III	2.20	4.35	0.0236	0.758	5.49%
UG I	2.07	4.48	0.0236	0.753	5.52%
Expt. ^a	2.2245	4.316			

^a Reference 13.

¹⁷ M. Sugawara, *Phys. Rev.* **117**, 614 (1950).

¹⁸ H. Feshbach, *Phys. Rev.* **107**, 1626 (1957).

¹⁹ R. Tamagaki and W. Watari, *Progr. Theoret. Phys. (Kyoto) Suppl.* **39**, 23 (1967).

TABLE V. Magnetic moments in nuclear magnetons and the quadrupole moment in F^{-2} .

Model	μ_0	$\Delta\mu_{LS}$	$\Delta\mu_p$	μ	Q
GS 2	0.8484	-0.0150	0.0010	0.8338	0.242
BS III	0.8478	-0.0051	0.0012	0.8445	0.259
UG I	0.8482	0.0068	0.0007	0.8556	0.280
Expt. ^a				0.8574	0.282

^a Reference 13.

tions, are almost the same for the three OBEP and are too small compared to the experimental magnetic moment. This means that the correction $\Delta\mu_{LS} + \Delta\mu_p$ must be positive. In Table V are given the values of μ_0 , $\Delta\mu_{LS}$, $\Delta\mu_p$, and μ_0 .

In Fig. 3 we show the values of $\phi(r)$ for the three OBEP. We see that the values of $\phi(r)$ differ appreciably in the three models, but the value of $\Delta\mu_p$ given in Table V, although positive, remains small and cannot by itself correct the value of the magnetic moment. Thus a correct magnetic moment can be a good test for the spin-orbit potential $V_{LS}(r)$ for isospin $T=0$ state. This has already been stressed by Tamagaki and Watari.¹⁹ Hence in order to get a correct magnetic moment, $V_{LS}(r)$ for $T=0$ must be rather positive. This potential is plotted in Fig. 4. From the three OBEP, only the UG potential has this property.

5. DEUTERON ELECTRIC QUADRUPOLE MOMENT

Knowing the deuteron wave function, we can calculate the electric quadrupole moment¹⁴

$$Q = (50)^{-1/2} \int (uw - 8^{-1/2}u^2)r^2 dr. \quad (18)$$

The value of the quadrupole moment depends sensi-

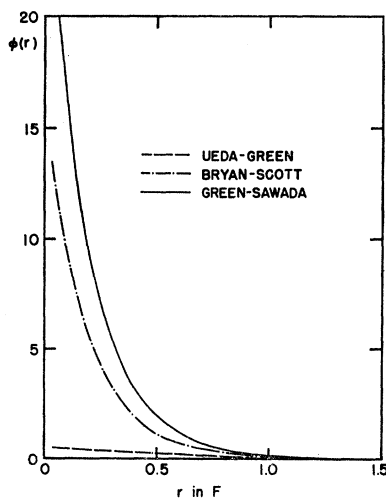


FIG. 3. Function $\phi(r)$ for $T=0$ states for the GS 2, BS III, and UG I models.

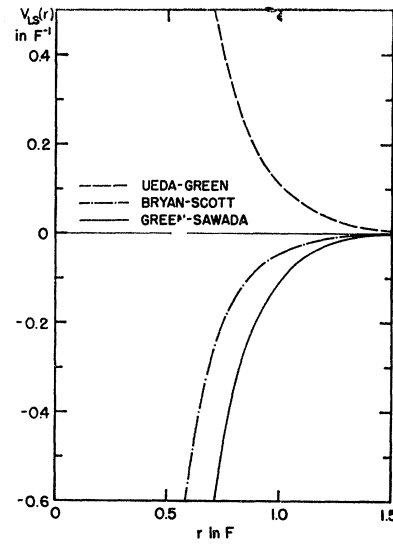


FIG. 4. $V_{LS}(r)$ potential for $T=0$ states, for the BS, GS 2, BS III, and UG I models.

tively on the value of the binding energy because a big part of the integral comes from the region where the wave functions are close to the asymptotic form. A rough estimate¹³ gives $Q \approx A/\sqrt{2}\gamma^2$, where A and γ are defined in Sec. 2. The computed values of the quadrupole moment Q are given in Table V.

6. DEUTERON FORM FACTORS

High-energy elastic scattering of electrons from deuterons provide information on various transforms of the deuteron wave function.²⁰⁻²⁴ Specifically, such experiments give information on

$$I_c(q) = \int (u^2 + w^2) j_0(x) dx \rightarrow 1, \quad (19)$$

$$I_Q(q) = \int 2w(u - 8^{-1/2}w) j_2(x) dx \rightarrow q^2 Q_d / 3\sqrt{2}, \quad (20)$$

$$I_{M_1}(q) = \int \left[\left(u^2 - \frac{w^2}{2} \right) j_0(x) + w(2^{-1/2}u + w^{-1}w) j_2(x) \right] dx \rightarrow 1 - \frac{3}{2}P_D, \quad (21)$$

$$I_{M_2}(q) = \frac{3}{4} \int w^2 [j_0(x) + j_2(x)] dx \rightarrow \frac{3}{4}P_D. \quad (22)$$

²⁰ V. Z. Jankus, Phys. Rev. **102**, 1586 (1956).

²¹ H. F. Jones, Nuovo Cimento **26**, 760 (1962).

²² M. Gourdin, Nuovo Cimento **35**, 1108 (1965).

²³ R. J. Adler, Ph.D. thesis, Stanford University, 1965 (unpublished).

²⁴ E. F. Erickson, Stanford University High-Energy Particle Laboratory Report No. 423, 1965 (unpublished).

Here $x = \frac{1}{2}q\sigma$, where q_e is close to q , the three-dimensional momentum transfer, for low q values (the arrows denote the limits as $q \rightarrow 0$) but departs from q at high values in different ways according to the theoretical treatment. Values of these integrals for the UG I wave function are given in Table VI.

The deuteron form factor can be written²⁴⁻²⁶

$$F^2 = f_E(\eta)(G_c^2 + G_Q^2) + f_M(\eta)(8/3)\eta G_M \times [1 + 2(1 + \eta) \tan^2 \frac{1}{2}\theta]. \quad (23)$$

Here $\eta = -l/4M_d^2$, where $-l$ is the four-momentum transfer squared and M_d is the mass of the deuteron, θ is the laboratory scattering angle of the electron, G_c , G_Q , G_M are the charge, quadrupole, and magnetic form factors of the deuteron, and $f_E(\eta)$ and $f_M(\eta)$ are quantities close to unity.

These form factors are connected with the deuteron wave-function transforms and the nucleon form factors²⁴

$$G_c = G_E^* I_c, \quad G_Q = G_E^* I_Q, \quad G_M = G_M^* I_{M_1} + G_E^* I_{M_2}, \quad (24)$$

and

$$G_E^* = G_E^p + G_E^n, \quad G_M^* = G_M + G_M^n, \quad (25)$$

where $G_E^* = G_E^p$ and G_M^p are charge and magnetic proton form factors, and G_E^n and G_M^n are the similar form factors of the neutron.

There are various fittings^{27,28} to the nucleon electromagnetic (E.M.) form factors G_E^* and G_M^* . In our computations we will use²⁷

$$2G_E^* = 2.50/(1 + q^2/15.7) - 1.60/(1 + q^2/26.7) + 0.10, \quad (26)$$

$$2G_M^* = 0.88[3.33/(1 + q^2/15.7) - 2.77/(1 + q^2/26.7) + 0.44], \quad (27)$$

where q is given in F^{-1} . The quantities $f_E(\eta)$ and $f_M(\eta)$ as well as certain relativistic corrections to G_c , G_Q , and G_M differ in various theoretical treatments.²¹⁻²⁴ However, the differences and the corrections themselves are

TABLE VI. Electromagnetic form-factor integrals I_c , I_Q , I_{m_1} , and I_{m_2} of the UG I model.

q^2	I_c	I_Q	I_{m_1}	I_{m_2}
1.0	0.6019	0.0381	0.5531	0.0357
2.0	0.4144	0.0556	0.3853	0.0316
3.0	0.3070	0.0632	0.2905	0.0283
4.0	0.2389	0.0663	0.2311	0.0256
5.0	0.1907	0.0673	0.1892	0.0233
6.0	0.1538	0.0672	0.1571	0.0213
7.0	0.1245	0.0665	0.1314	0.0196
8.0	0.1009	0.0653	0.1106	0.0181
9.0	0.0821	0.0638	0.0939	0.0167

²⁵ D. J. Drickey and L. N. Hund, Phys. Rev. Letters **9**, 521 (1962).

²⁶ D. Benaksas *et al.*, Phys. Rev. **148**, 1327 (1966).

²⁷ T. Jansens *et al.*, Phys. Rev. **142**, 992 (1966).

²⁸ L. H. Chan *et al.*, Phys. Rev. **141**, 1248 (1966).

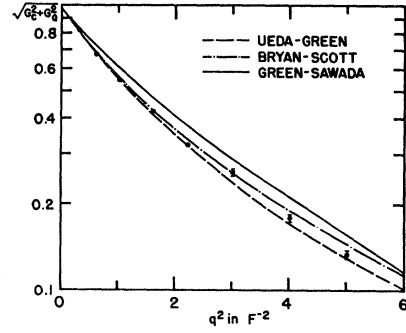


FIG. 5. Electromagnetic form factor $[G_c^2(q) + G_Q^2(q)]^{1/2}$ of the deuteron as a function of the momentum transfer, calculated from the BS, GS, and UG potentials. The experimental data are those of D. J. Drickey and L. N. Hund (Ref. 25) (solid circles) and of D. Benaksas *et al.* (Ref. 26) (solid squares).

small for $q \leq 2$ F. In this region $\eta \approx q^2/4M_d^2$, where $M_d^2 = 90.3$ F^{-2} .

The calculated values of the deuteron electric form factor $(G_c^2 + G_Q^2)^{1/2}$ for the GS 2, BS III, and UG I models are shown in Fig. 5.

7. SUMMARY AND DISCUSSION

We have seen that realistic OBEP describe quite well the low-energy properties of the $N-N$ interaction. This is rather satisfying since the parameters of these models had primarily been adjusted to fit the $10 \leq E \leq 350$ MeV phenomenological phase shifts. The UG I and BS III models give rather good fits to the effective-range expansion parameters, the binding energy of the deuteron, and the electromagnetic form factors of the deuteron. The difficulty with GS 2 largely relates to the rather high deuteron binding energy and in part reflects the compromises made in adjusting only two parameters. It should be noted that the GS seven-parameter models are more comparable to UG I (seven parameters) and BS III (10 parameters).

Only the UG model gives a good fit to the measured magnetic moment. This improvement apparently comes from the sign of the $V_{LS}(r)$, suggesting that in the $T=0$ state V_{LS} must be positive. The main differences in three OBEP models that affect the behavior of the V_{LS} for $T=0$ are two effects due to the ρ meson: (i) It increases the value of $V_{LS}(r)$ and (ii) it decreases the value of $\phi(r)$ for $T=0$. From Table I of Ref. 5, we see that the contribution to $V_{LS}(r)$ is proportional to $g^2(1 + \frac{1}{3}f/g)^2$, which is about 23 for the GS model, 39 for the BS model, and about 123 for the UG model.

The quadrupole moment is quite sensitive to the potential model as long as the binding energy has a correct value. In turn, the binding energy is very sensitive to the parameters of the model. We expect that a small change in the parameters of the UG I model will lead to a correct value of the binding energy, from 2.07 to 2.22 MeV, without significantly affecting the fit to the

phase shifts. For binding energy 2.22 MeV our calculations indicate the UG model would give $Q=0.276 F^2$.

In closing, it must be remarked that we have come amazingly far with OBEP. When the OBE model was initially developed in 1961, S waves could not be treated and the various unitarization schemes were of dubious validity even for the P and D waves. With the use of regularization techniques and the incorporation of velocity-dependent terms, the OBE model in the form of the potential-model approach has taken on very realistic features. The fact that with 5–10 adjustable parameters one can now do well in accounting for 25 phase-shift functions over a broad energy region (10–350 MeV) and at the same time account for about four low-energy parameters is quite satisfying. It is quite likely that further progress on the N - N interaction can be made by further testing and adjustments of the model

to additional types and ranges of experimental data. Were the objective of such efforts viewed from the standpoint of particle physics where the N - N interaction is but one of many possible baryon-baryon interactions, such tedious endeavors might not be worth while. However, when viewed from the standpoint of nuclear physics for which the N - N interaction plays such a fundamental role, we believe that such painstaking endeavors will bring commensurate increases in our understanding of the entire field of nuclear physics.

ACKNOWLEDGMENTS

The writers would like to thank Dr. T. Sawada, Dr. T. Ueda, and Dr. A. Dainis for many helpful discussions. We also thank Dr. R. A. Bryan and Dr. R. L. Scott for sending us a paper prior to publication.

Alpha-Particle Yields and Angular Distributions in the $O^{16}(Li^6, \alpha_0)F^{18}$ Reaction from 4.8 to 13.8 MeV*

M. WAYNE GREENE†

Department of Physics and Astronomy, Iowa City, Iowa 52240

(Received 31 January 1968; revised manuscript received 21 June 1968)

The yield and angular distributions of α particles from the $O^{16}(Li^6, \alpha_0)F^{18}$ reaction were measured for the bombarding range 4.8 to 13.8 MeV. Nine distinct peaks were observed in the yield curve measured at 0° and had peak-to-valley ratios varying from 1.3 to 6.0. A fluctuation analysis of the yield curve gives a corrected coherence width $\Gamma=0.49\pm 0.40$ MeV (c.m. system) in the excitation energy range of Na^{22} of 18.0 to 24.6 MeV for the sample size $n=5.3$. This analysis predicts a direct reaction contribution to the differential cross section of 0 to 60%. Angular distributions were measured at seven energies: 5.50, 5.70, 6.22, 11.60, 12.20, 12.80, and 13.30 MeV, which correspond to peak and valley energies observed in the yield curve. At the three lowest bombarding energies, the angular distributions have little structure, while at the four higher energies they oscillate rapidly.

I. INTRODUCTION

EVIDENCE for both compound nucleus and direct interaction has been observed in lithium-induced reactions,¹ particularly in the $C^{12}+Li^6$ investigations,²⁻⁷ in the Li^6+Be^9 investigations,^{8,9} and in the Li^6+Be^9

investigations.⁹ A summary of these results has been given recently by Carlson.¹⁰

A fluctuation study of several reaction particle groups from the Li^6+C^{12} reaction⁵ over the bombarding range 2.4 to 8.5 MeV suggested that more than 40% of the interaction cross section was due to compound-nucleus formation. The average energy level width was found to be 250 keV at 17-MeV excitation in the compound nucleus F^{18} . Fluctuation analyses have also been applied by Seale⁹ to the $Li^6+Be^9 \rightarrow p+C^{14}$ and $Li^6+B^{10} \rightarrow \alpha+C^{12}$ reactions. Little structure was observed in the yield curve for the first reaction over the bombarding range 3.8 to 6.4 MeV. In the second reaction, the bombarding range was much larger (3.2 to 13.6 MeV), and even over this large range, the sample size was small: $n\sim 2.5$. In the latter reaction, the average

* This work was supported by the National Science Foundation.

† Now at Chadwick Laboratory, University of Liverpool, Liverpool 3, England.

¹ G. C. Morrison and M. N. Huberman, in *Proceedings of the Second Conference on Reactions between Complex Nuclei, 1960*, edited by A. Zucker, E. C. Halbert, and F. T. Howard (John Wiley & Sons, Inc., New York, 1960), p. 246; Phys. Rev. **129**, 791 (1963).

² R. K. Hobbie and F. F. Forbes, Phys. Rev. **126**, 2137 (1962).

³ J. M. Blair and R. K. Hobbie, Phys. Rev. **128**, 2282 (1962).

⁴ D. W. Heikkinen, Phys. Rev. **141**, 1007 (1966).

⁵ T. G. Dzubay, Phys. Rev. **158**, 977 (1967).

⁶ D. J. Johnson, M.S. thesis, University of Iowa, 1967 (unpublished).

⁷ K. Bethge, K. Meier-Ewert, K. Pfeiffer, and R. Bock, Phys. Letters **24B**, 663 (1967).

⁸ R. L. McGrath, Phys. Rev. **145**, 802 (1966).

⁹ W. A. Seale, Phys. Rev. **160**, 890 (1967).

¹⁰ R. R. Carlson, in *Nuclear Research with Low Energy Accelerators*, edited by J. B. Marion and D. M. Van Patter (Academic Press Inc., New York, 1967).